



Calhoun: The NPS Institutional Archive
DSpace Repository

Theses and Dissertations

Thesis and Dissertation Collection

1986-09

A correlation for the heat transfer coefficient in a rectangular passage containing protuberance

Cesur, Ceyhun

<http://hdl.handle.net/10945/21748>

Downloaded from NPS Archive: Calhoun



Calhoun is a project of the Dudley Knox Library at NPS, furthering the precepts and goals of open government and government transparency. All information contained herein has been approved for release by the NPS Public Affairs Officer.

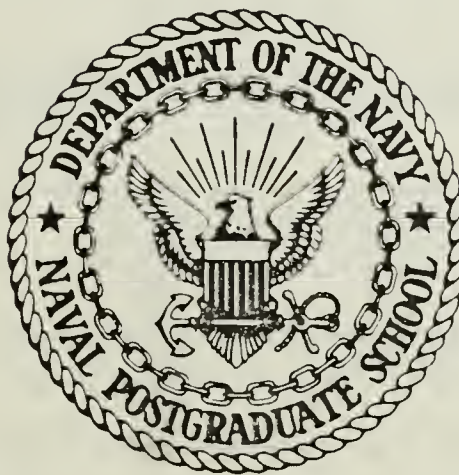
Dudley Knox Library / Naval Postgraduate School
411 Dyer Road / 1 University Circle
Monterey, California USA 93943

<http://www.nps.edu/library>

DUDLEY KNOX LIBRARY
NAVAL POSTGRADUATE SCHOOL
MONTEREY CALIFORNIA 93943-5002

NAVAL POSTGRADUATE SCHOOL

Monterey, California



THESIS

A CORRELATION FOR THE HEAT TRANSFER
COEFFICIENT IN A RECTANGULAR
PASSAGE CONTAINING PROTUBERANCE

by

Ceyhun Cesur

September 1986

Thesis Advisor:

Allan D. Kraus

Approved for public release; distribution is unlimited.

T230163

THE UNIVERSITY OF CHICAGO

LIBRARY



EX-107



EX-107

REPORT DOCUMENTATION PAGE

REPORT SECURITY CLASSIFICATION UNCLASSIFIED		1b. RESTRICTIVE MARKINGS		
SECURITY CLASSIFICATION AUTHORITY		3 DISTRIBUTION/AVAILABILITY OF REPORT Approved for public release; distribution is unlimited		
DECLASSIFICATION/DOWNGRADING SCHEDULE				
PERFORMING ORGANIZATION REPORT NUMBER(S)		5 MONITORING ORGANIZATION REPORT NUMBER(S)		
NAME OF PERFORMING ORGANIZATION Naval Postgraduate School		6b OFFICE SYMBOL (If applicable) 69	7a. NAME OF MONITORING ORGANIZATION Naval Postgraduate School	
ADDRESS (City, State, and ZIP Code) Monterey, California 93943-5000		7b. ADDRESS (City, State, and ZIP Code) Monterey, California 93943-5000		
NAME OF FUNDING/SPONSORING ORGANIZATION		8b. OFFICE SYMBOL (If applicable)	9 PROCUREMENT INSTRUMENT IDENTIFICATION NUMBER	
ADDRESS (City, State, and ZIP Code)		10 SOURCE OF FUNDING NUMBERS		
		PROGRAM ELEMENT NO	PROJECT NO	
		TASK NO	WORK UNIT ACCESSION NO	
TITLE (Include Security Classification) A CORRELATION FOR THE HEAT TRANSFER COEFFICIENT IN A RECTANGULAR PASSAGE CONTAINING PROTUBERANCE				
PERSONAL AUTHOR(S) Cesur, Ceyhun				
11 TYPE OF REPORT Master's Thesis	13b TIME COVERED FROM TO	14 DATE OF REPORT (Year, Month, Day) 1986 September	15 PAGE COUNT 58	
SUPPLEMENTARY NOTATION				
COSATI CODES		18 SUBJECT TERMS (Continue on reverse if necessary and identify by block number) Heat exchanger, convective heat-transfer coefficient.		
FIELD	GROUP			SUB-GROUP
ABSTRACT (Continue on reverse if necessary and identify by block number) An experimental investigation was carried out to determine the effect on the convective heat transfer coefficient of protuberances in a rectangular passage. A cross-flow compact type heat exchanger formed by several parallel spaced plates including protuberances was tested by using water, glycol and air as a working fluids. Heat transfer coefficient data was obtained by measuring mass flow-rate, temperature and pressure drops across the heat exchanger. Heat transfer characteristics are discussed and correlations for Nusselt number, Colburn factor and friction factor have been obtained.				
DISTRIBUTION/AVAILABILITY OF ABSTRACT <input checked="" type="checkbox"/> UNCLASSIFIED/UNLIMITED <input type="checkbox"/> SAME AS RPT <input type="checkbox"/> DTIC USERS		21 ABSTRACT SECURITY CLASSIFICATION UNCLASSIFIED		
NAME OF RESPONSIBLE INDIVIDUAL Prof. Allan D. Kraus		22b TELEPHONE (Include Area Code) (408) 646-649-8276	22c OFFICE SYMBOL Code 69Ks	

Approved for public release; distribution is unlimited.

A Correlation For The Heat Transfer Coefficient In A Rectangular
Passage Containing Protuberance.

by

Ceyhun Cesur
Lieutenant JG, Turkish Navy
B.S., Turkish Naval Academy 1980

Submitted in partial fulfillment of the
requirements for the degree of

MASTER OF SCIENCE IN MECHANICAL ENGINEERING

from the

NAVAL POSTGRADUATE SCHOOL
September 1986

ABSTRACT

An experimental investigation was carried out to determine the effect on the convective heat transfer coefficient of protuberances in a rectangular passage.

A cross-flow compact type heat exchanger formed by several parallel spaced plates including protuberances was tested by using water, glycol and air as a working fluids. Heat transfer coefficient data was obtained by measuring mass flow-rate, temperature and pressure drops across the heat exchanger.

Heat transfer characteristics are discussed and correlations for Nusselt number, Colburn factor and friction factor have been obtained.

1/10/20
C338915
2.1

TABLE OF CONTENTS

I.	INTRODUCTION	4
A.	BACKGROUND	11
B.	THESIS OBJECTIVES	11
II.	THEORY OF OPERATION	13
A.	GENERAL	13
B.	INDIVIDUAL AND OVERALL HEAT TRANSFER COEFFICIENTS	13
C.	HEAT TRANSFER COEFFICIENT DEPENDENCES	16
D.	HEAT TRANSFER COEFFICIENT LIMITATIONS	16
III.	THE EMPIRICAL CORRELATION FOR THE CONVECTIVE HEAT TRANSFER COEFFICIENT	18
IV.	EXPERIMENTAL PROCEDURE	22
A.	EXPERIMENTAL PROCEDURE	22
	1. Heat Exchanger	22
	2. Geometric Properties Of The Heat Exchanger	24
	3. Instrumentation	28
V.	CONCLUSIONS AND RECOMMENDATIONS	29
A.	CONCLUSIONS	29
B.	RECOMMENDATIONS	29
APPENDIX A:	SAMPLE CALCULATIONS	30
1.	CONSTANT VALUES	30
2.	SAMPLE CALCULATIONS	31
a.	CALCULATION PROCEDURE	31
b.	HOT WATER-COLD WATER STUDY	33
c.	HOT GLYCOL-COLD WATER STUDY	33
d.	HOT WATER-COLD AIR STUDY	33
e.	CALCULATION OF CORRELATIONS	33

APPENDIX B: DIMENSIONAL ANALYSIS	50
APPENDIX C: UNCERTAINTY ANALYSIS	53
LIST OF REFERENCES	56
INITIAL DISTRIBUTION LIST	57

LIST OF TABLES

1.	THE EXPERIMENTAL DATA FOR THE WATER-WATER STUDY	36
2.	PROPERTIES OF THE HOT WATER	37
3.	SOME RESULTS OF THE WATER-WATER STUDY	38
4.	SOME RESULTS OF THE WATER-WATER STUDY	39
5.	THE EXPERIMENTAL DATA FOR THE GLYCOL-WATER STUDY	40
6.	PROPERTIES OF THE HOT GLYCOL	41
7.	SOME RESULTS OF THE GLYCOL-WATER STUDY	42
8.	SOME RESULTS OF THE GLYCOL-WATER STUDY	43
9.	THE EXPERIMENTAL DATA FOR THE WATER-AIR STUDY	44
10.	SOME RESULTS OF THE WATER-AIR STUDY	45
11.	SOME RESULTS OF THE WATER-AIR STUDY	46
12.	VARIABLES FOR CONVECTION	50

LIST OF FIGURES

2.1	Temperature distribution in the neighborhood of a tube wall.	14
3.1	Experiment for measuring the average convection heat transfer coefficient.	18
3.2	Dimensionless representation of convection heat transfer measurements.	20
3.3	Dimensionless representation of convection heat transfer measurements.	21
4.1	Schematic diagram of the experimental system.	23
4.2	Schematic view of the heat exchanger.	25
4.3	A detached edge view of the top plate configuration.	26
4.4	A detached edge view of another type of configuration.	26
4.5	A detached edge view of another type of configuration.	26
4.6	A detached edge view of the bottom plate configuration.	26
4.7	The plate configurations in the heat exchanger.	27
A.1	A correlation for the Nusselt number.	47
A.2	A correlation for the Colburn factor.	48
A.3	A correlation for the friction factor.	49

NOMENCLATURE

A : Heat transfer surface area	$[m^2]$
A_{bb} : Bump base area	$[m^2]$
A_{bc} : Bump cross sectional area	$[m^2]$
A_{bs} : Bump surface area	$[m^2]$
A_f : Passage flow area	$[m^2]$
A_s : Plate surface area	$[m^2]$
b : Bump base diameter	$[m]$
C_c : Cold fluid capacity rate	$[J/kgs]$
C_h : Hot fluid capacity rate	$[J/kgs]$
C_r : Capacity rate ratio	
C_p : Specific heat at constant pressure	$[J/kgK]$
D : Equivalent diameter	$[m]$
f : Friction factor	
G : Mass velocity	$[kg/m^2s]$
h : Heat transfer coefficient	$[W/m^2K]$
h_b : Bump height	$[m]$
j : Colburn factor	
k : Thermal conductivity	$[W/mK]$
K_c : Contraction loss coefficient	
K_e : Expansion loss coefficient	
L : Plate length	$[m]$
m : Fluid mass flow rate	$[kg/s]$
N : Bump numbers	
N_{tu} : Number of transfer units	
Nu : Nusselt number	
P : Wetted perimeter	$[m]$
Pr : Prandtl number	
Q : Heat tranfer from hot fluid to cold fluid	$[W]$
q'' : Heat flux	$[W/m^2]$
Re : Reynolds number	
r_w : Wall resistance	$[W/m^2K]$
s : Arc length of the bump	$[m]$
St : Stanton number	

T : Hot fluid temperature	[C]
t : Cold fluid temperature	[C]
T_b : Hot fluid bulk temperature	[C]
t_c : Cold fluid bulk temperature	[C]
\overline{T} : Hot fluid average temperature	[C]
\overline{t} : Cold fluid average temperature	[C]
T_s : Plate surface temperature	[C]
t_p : Passage height	[m]
U : Overall heat transfer coefficient	[W/m ² K]
V : Fluid velocity	[m/s]
v : Specific volume	[m ³ /kg]
w : Plate width	[m]
ΔT : Temperature drop	[C]
ρ : Fluid density	[kg/m ³]
δ : Material thickness	[m]
ν : Kinematic viscosity	[m ² /s]
μ : Dynamic viscosity	[Ns/m ²]
μ_w : Dynamic viscosity at wall temperature	[Ns/m ²]
ε : Exchanger effectiveness	
σ : Ratio of free flow area to frontal area	

Subscripts :

c : cold fluid
h : hot fluid
1 : inlet
2 : outlet

ACKNOWLEDGEMENTS

The author would like to express his appreciation to Professor Allan D. Kraus for his guidance and friendship in completing this work. Many thanks are due to several people whose helpful interest and technical advice contributed in the construction of the experimental system.

I. INTRODUCTION

A. BACKGROUND

In a heat exchanger, one of the important parameters controlling the net heat transfer from the hot fluid to the cold fluid is the surface area separating the two fluids across which the heat transfer takes place. When large quantities of heat are to be transferred, computations usually indicate a requirement for large heat transfer surface areas. Increasing the area necessarily means either increasing the total path length travelled by the fluids in the heat exchanger or simultaneously decreasing the diameter of tubes and increasing the number of tubes.

Where high volume is not a limiting constraint, flat plates can be employed. However, use of flat plates to obtain the necessary surface may involve other heat transfer considerations in the device.

In order to enhance the heat transfer characteristics of flat plate exchangers, some type of obstruction may be placed between the plates in order to cause the fluids to take a sinuous path between them. These obstructions are often in the form of a honeycomb structure but they inherently possess several problems. First, there is usually a straight path through the heat exchanger in the direction of flow thereby defeating the purpose of the obstructions. In addition, the sharp bends and corners in the honeycomb structure can create undesirable dead spots within the heat exchanger. They may also represent weak points and areas of deleterious stress concentration in the structure which, upon heating and cooling, will often crack.

Interest in heat exchanger surfaces with a high ratio of heat transfer area to core volume is increasing at an accelerated pace. The primary reasons for the use of these more compact surfaces is that smaller, lighter-weight, and lower cost heat exchangers are the result. These gains are brought about both by the direct geometric advantage of higher 'area density' and also a higher heat transfer coefficient for the smaller flow passages.

B. THESIS OBJECTIVES

The objective of this thesis is to determine the effect of protuberances in a rectangular passage on the convective heat transfer coefficient.

In order to accomplish this objective, measurements of fluid mass flow-rate, inlet and outlet temperatures and exchanger pressure drops were obtained for several different fluids flowing in a cross-flow compact type heat exchanger containing the protuberances. Heat transfer coefficients were then obtained. From these data, correlations for Nusselt number, Colburn factor and friction factor were then developed.

II. THEORY OF OPERATION

A. GENERAL

The rate of heat transfer between a solid surface and a fluid can be expressed in much the same way as for simple heat conduction through solids:

$$Q = h A \Delta T \quad (\text{eqn 2.1})$$

Here ΔT is the temperature drop between the bulk fluid and the wall, A is the heat transfer surface area and h is the heat transfer coefficient. The last term is equivalent to the term k/L in the simple heat conduction equation.

Equation (2.1), which is often referred to as "*Newton's Law of Cooling*" is easy to use except for the evaluation of the heat transfer coefficient h , which depends on the fluid flow conditions, the thermal properties of the fluid, and the passage size.

It is often convenient in heat exchanger work to combine the two surface heat transfer coefficients (that is, for the hot and cold fluid streams) and the thermal resistance of the tube wall to give a single parameter: the overall heat transfer coefficient, U , which may be defined as

$$U = Q / A \Delta T \quad (\text{eqn 2.2})$$

B. INDIVIDUAL AND OVERALL HEAT TRANSFER COEFFICIENTS

Equation (2.2) may be written in another form :

$$q'' = U (T_1 - T_2) \quad (\text{eqn 2.3})$$

Here q'' is the heat flux from stream-1 to stream-2, having bulk temperatures T_1 and T_2 and U is the overall heat transfer coefficient.

It is now time to consider the questions of what precisely is meant by the interface area, and what is the relation of U to the individual resistances to heat transfer represented by the solid wall separating the two fluids, the deposits of dirt that

may cling to the surfaces of the wall, and the low-velocity fluid films that adjoin those deposits or the wall itself.

Fig. 2.1 illustrates the temperature profile discontinuities at locations a (inner surface of inner deposit), b (outer surface of inner deposit and inner surface of tube wall), c (outer surface of tube wall and inner surface of outer deposit), d (outer surface of outer deposit). It can also be seen that the fluid temperatures lie both above and below T_a and T_b , for these are defined as flow averages, that is, averages for the duct cross sections in which each element of area is weighted by the specific heat C_p times the local mass flow rate ρV .

Thus,

$$T_{1or2} = \left(\int \rho C_p V T \partial s / \int \rho C_p V \partial s \right)_{1or2} \quad (\text{eqn 2.4})$$

where the averages are taken over the whole of the cross section of the ducts in question.

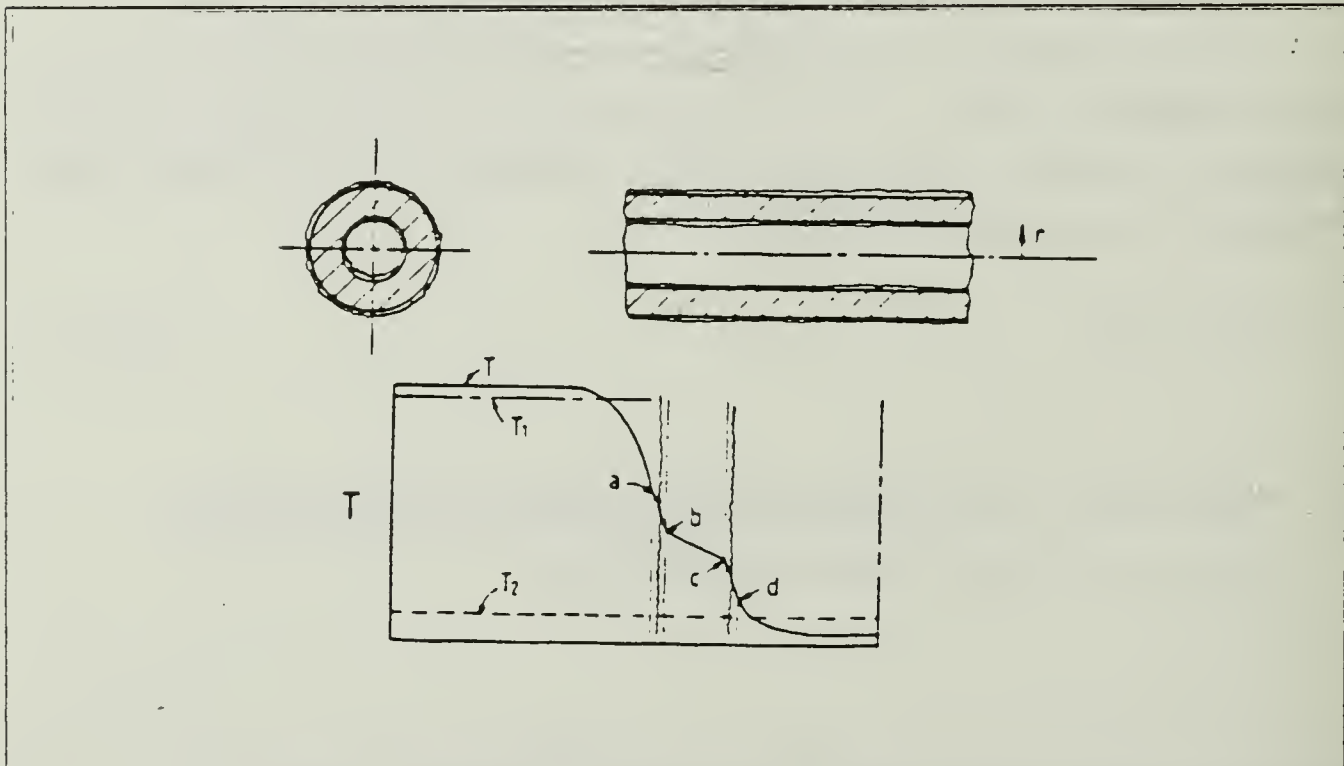


Figure 2.1 Temperature distribution in the neighborhood of a tube wall.

Let h_{1a} and h_{d2} now represent the film heat transfer coefficient on the inside and outside of the tube, respectively; let h_{ab} and h_{cd} represent heat transfer coefficients for

the two dirt deposits; and h_{bc} represents the heat transfer coefficient for the tube wall itself. h_{ab} , h_{bc} , and h_{cd} will all be related to the relevant material thickness δ and thermal conductivities k by

$$h_{ab} = k_{ab} / \delta_{ab} \quad (\text{eqn 2.5})$$

$$h_{bc} = k_{bc} / \delta_{bc} \quad (\text{eqn 2.6})$$

$$h_{cd} = k_{cd} / \delta_{cd} \quad (\text{eqn 2.7})$$

Each heat transfer coefficient, to be meaningful, must be associated with an area A . When this is done, the fact that the heat flow through all the elements in question is the same leads to

$$\begin{aligned} U A (T_1 - T_2) &= h_{1a} A_{1a} (T_1 - T_a) \\ &= h_{ab} A_{ab} (T_a - T_b) \\ &= h_{bc} A_{bc} (T_b - T_c) \\ &= h_{cd} A_{cd} (T_c - T_d) \\ &= h_{d2} A_{d2} (T_d - T_2) \end{aligned} \quad (\text{eqn 2.8})$$

Here A_{ab} , A_{bc} , A_{cd} can most appropriately be taken as the arithmetic means of the inner and outer surface areas of the materials in question; and A_{1a} and A_{d2} are best taken as the surface areas pertaining to locations a and d respectively. The area A without subscript, associated with U , requires arbitrary definition; it can be set equal to any of the other areas.

Elimination T_a , T_b , T_c , and T_d now leads to the following important connection between the overall coefficient U and the individual coefficients

$$U = [(A / h_{1a} A_{1a}) + (A / h_{ab} A_{ab}) + (A / h_{bc} A_{bc}) + (A / h_{cd} A_{cd}) + (A / h_{d2} A_{d2})]^{-1} \quad (\text{eqn 2.9})$$

Evidently, the relationship is best understood as implying that the reciprocal of UA is the overall resistance to heat transfer, and that the overall resistance is equal to the sum of the individual resistances $(h_{1a}A_{1a})^{-1}$, $(h_{ab}A_{ab})^{-1}$, and

In the case of heat transfer across a plane wall, all the areas take identical values. Then Equation (2.9) reduces to

$$U = [(1/h_{1a}) + (1/h_{ab}) + (1/h_{bc}) + (1/h_{d2})]^{-1} \quad (\text{eqn 2.10})$$

C. HEAT TRANSFER COEFFICIENT DEPENDENCES

A dimensional analysis easily shows that the heat transfer coefficient may be found to be related to two dimensionless parameters : the Nusselt and Prandtl numbers. The Nusselt number, Nu , is the term used for the grouping hL/k , where L is a typical length dimension that pertains to the apparatus, and k is the thermal conductivity of the fluid. This quantity is the ratio of the heat transfer coefficient to the thermal conductance implied by the quantity k/L . It can be seen intuitively, from the simple conduction equation, that the heat flow rate to a fluid flowing through a passage should be proportional to the thermal conductivity divided by a representative distance in the direction of heat flow such as the passage equivalent diameter.

Obviously, further prescription is needed of precisely what dimension is in question (such as duct diameter), and just where the thermal conductivity is to be measured (such as at the interface, at the bulk condition, or in some reference state).

The Prandtl number, Pr , is the term used for the ratio $C_p\mu/k$. This quantity is the ratio of the molecular diffusivity of momentum (as indicated by the viscosity) to the molecular diffusivity of heat (as indicated by the ratio of the thermal conductivity to the specific heat).

D. HEAT TRANSFER COEFFICIENT LIMITATIONS

The concept of the heat transfer coefficient is so convenient, and so reminiscent of electrical circuit theory, that there is some danger that its validity may be presumed to be unlimited. A few remarks on its limitations are therefore in order.

First, the heat flux (to or from the fluids) may not be proportional to the temperature difference alone. Other examples can be found, for example, those involving chemical reaction rather than phase change.

Second, the value of the coefficient is by no mean independent of the values of the property differences that multiply it. In the case of heat transfer by natural convection, it is well known that the coefficient increases with the imposed temperature difference.

Third, there are circumstances in which nonuniformities of temperature or concentration along the interface are so steep as to affect the value of the transfer coefficient. In these circumstances, it may be best to work with the fluxes and property differences directly, avoiding all reference to coefficients.

III. THE EMPIRICAL CORRELATION FOR THE CONVECTIVE HEAT TRANSFER COEFFICIENT

The manner in which a convection heat transfer coefficient may be obtained experimentally is illustrated in Fig. 3.1. In a prescribed geometry, such as a flat plate in parallel flow, convection heat transfer occurs from the plate to the fluid, if the surface of the plate is at a higher temperature than that of the fluid.

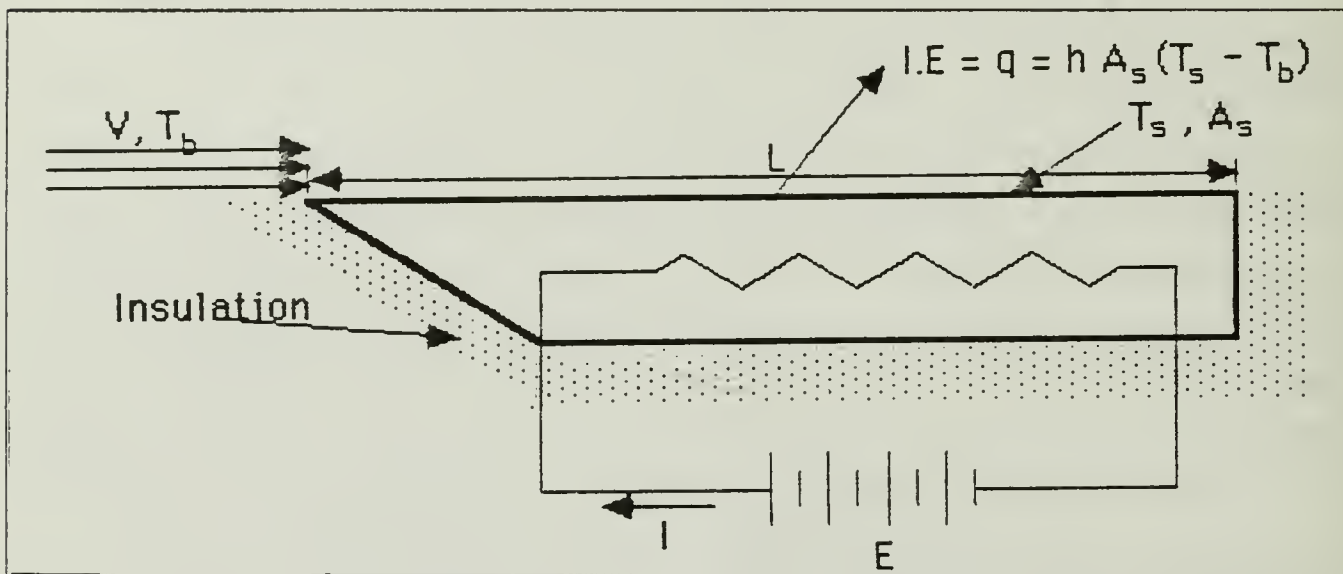


Figure 3.1 Experiment for measuring the average convection heat transfer coefficient.

The convection heat transfer coefficient h , which is an average associated with the entire plate, can be computed from *Newton's law of cooling*,

$$Q = h A_s (T_s - T_b) \quad (\text{eqn 3.1})$$

where

h : average convective coefficient	$[W/m^2K]$
A_s : plate surface area	$[m^2]$
T_s : plate surface temperature	$[C]$
T_b : fluid bulk temperature	$[C]$

From a knowledge of the characteristic length L and the fluid properties, the Nusselt, Reynolds, and Prandtl numbers can be computed from their definitions. The Nusselt number is a function of the Reynolds and Prandtl numbers.

$$Nu = (h L / k) = f(Re, Pr) \quad (\text{eqn 3.2})$$

and

$$Re = V L / \nu \quad (\text{eqn 3.3})$$

$$Pr = C_p \mu / k \quad (\text{eqn 3.4})$$

where

L : characteristic length	[m]
k : thermal conductivity	[W/mK]
V : fluid velocity	[m/s]
μ : fluid dynamic viscosity	[Ns/m ²]
C_p : specific heat	[J/kgK]
ν : fluid kinematic viscosity	[m ² /s]

The forgoing procedure is reproducible for a variety of test conditions. One can vary the velocity V and the plate length L , as well as the nature of the fluid, using for example air, water and glycol, which have substantially different Prandtl numbers. We would then be left with many different values of the Nusselt numbers corresponding to a wide range of Reynolds and Prandtl numbers and the results could be plotted on *log-log* scale, as shown in Fig. 3.2.

Each symbol represents a unique set of test conditions. As is often case, the results associated with a given fluid, and hence a fixed Prandtl number, fall close to a straight line, which may be represented by an algebraic expression of the form
 Since the values of C , m and n are independent of the nature of the fluid, the family of straight lines corresponding to different Prandtl numbers can be collapsed to a single line by plotting the results in terms of the ratio, Nu/Pr^n , as shown in Fig. 3.3.

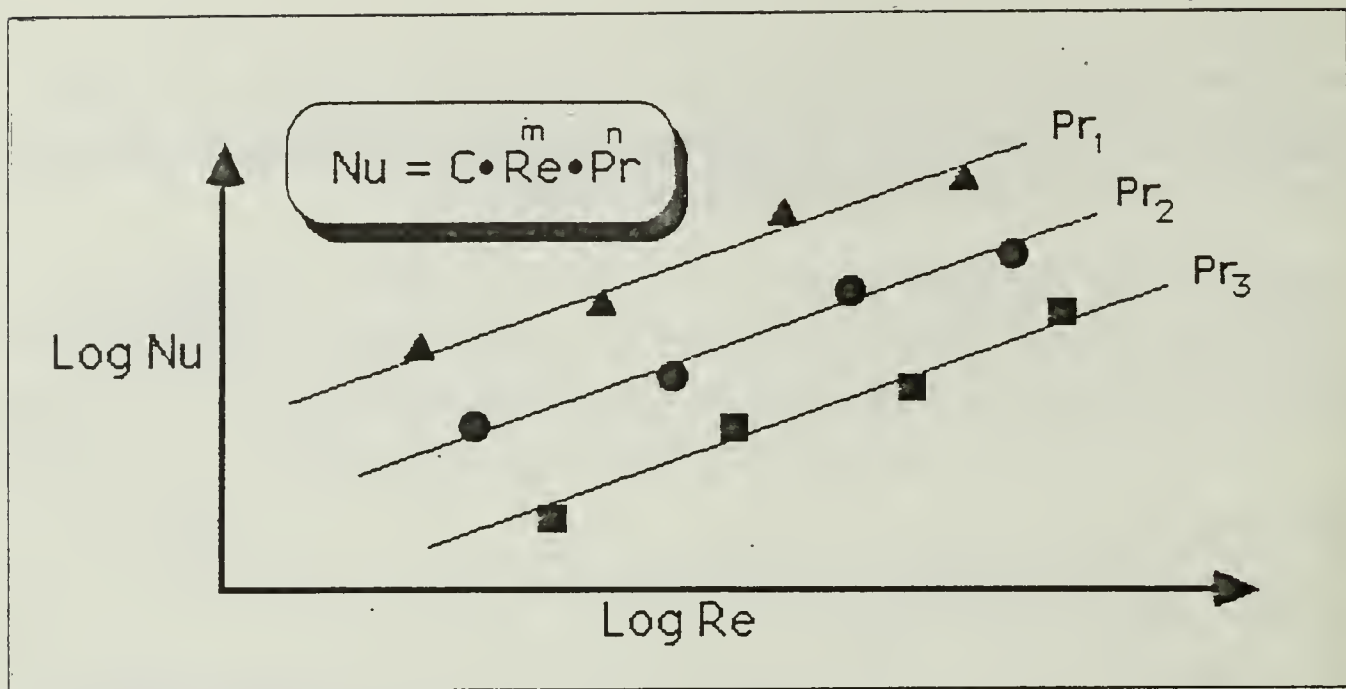


Figure 3.2 Dimensionless representation of convection heat transfer measurements.

$$Nu = C Re^m Pr^n \quad (\text{eqn 3.5})$$

Because Equation (3.5) is inferred from experimental measurements, it is termed an empirical correlation. However, the specific values of coefficient C and the exponents m and n vary with the nature of the surface geometry and the type of flow.

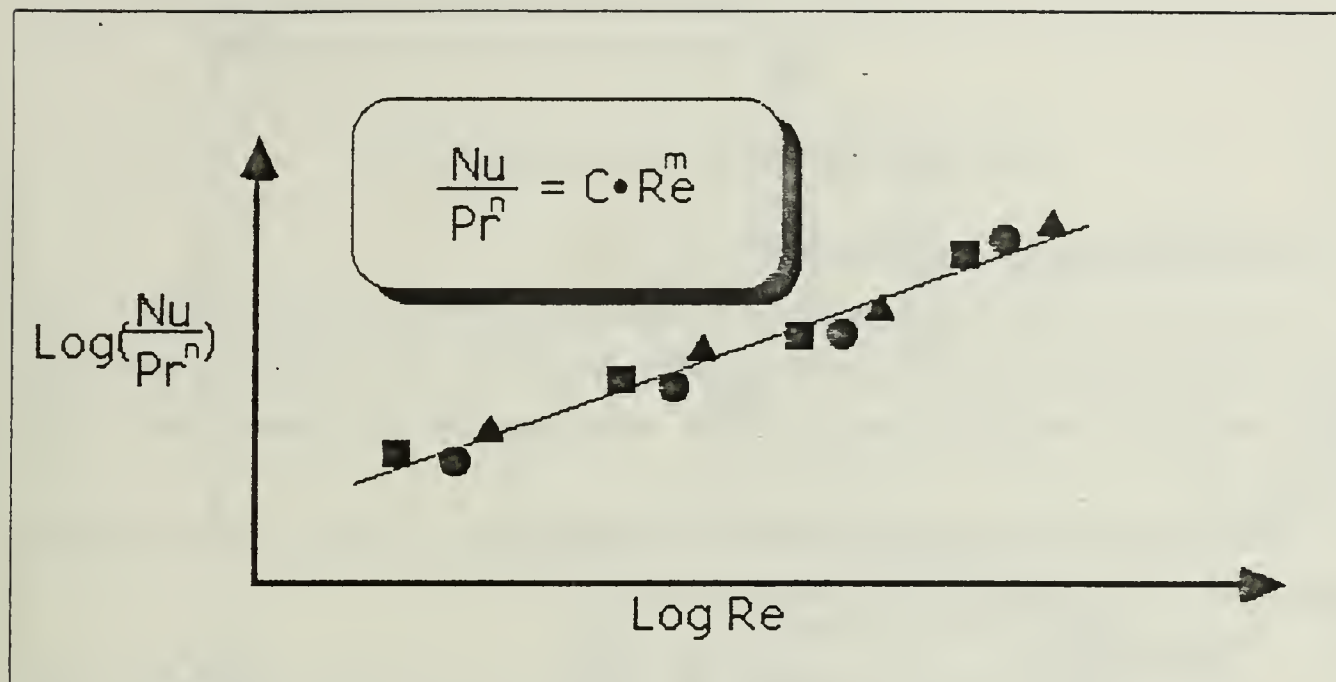


Figure 3.3 Dimensionless representation of convection heat transfer measurements.

IV. EXPERIMENTAL PROCEDURE

A. EXPERIMENTAL PROCEDURE

To reach the thesis objectives an experimental system was established. It is shown schematically in Fig. 4.1, and using water, glycol and air as a working fluids, the effect upon the convective heat transfer coefficient by the protuberances was investigated.

The physical configuration of the heat exchanger and some instrumentation methods will be discussed in the following sections.

1. Heat Exchanger

The heat exchanger (Fig. 4.2) was formed by 14 parallel spaced plates with the spaces between the plates defining fluid passages. The plates are totally nested with each other to provide, by minimizing unsupported areas, a structurally sounder device.

When the fluids enter the passage, they are confronted with a unique pattern of interfering protuberances which come downward from the plate above and upward from the plate below. The turbulence created as the fluids make their sinuous path from inlet to outlet greatly enhances the heat transfer characteristics. Moreover, the fact that the rounded protuberances nest within each other and actually engage the adjacent plate gives the heat exchanger structural rigidity which permits the use of thinner metallic plate material. This further enhances the heat transfer characteristics by lowering the metal resistance to heat flow.

A brief description of the figures now follows :

Fig. 4.2.a is an external view of the heat exchanger.

Fig. 4.2.b is an internal view of the heat exchanger.

Fig. 4.3 is a detached edge view of the top plate configuration employed in the heat exchanger.

Fig. 4.4, and Fig. 4.5 are detached edge views of another type of configuration employed in the heat exchanger.

Fig. 4.6 is a detached edge view of the bottom plate configuration employed in the heat exchanger.

Fig. 4.7 is a view taken substantially along line a-a of Fig. 4.2, and shows the configurations of the plates in the heat exchanger.

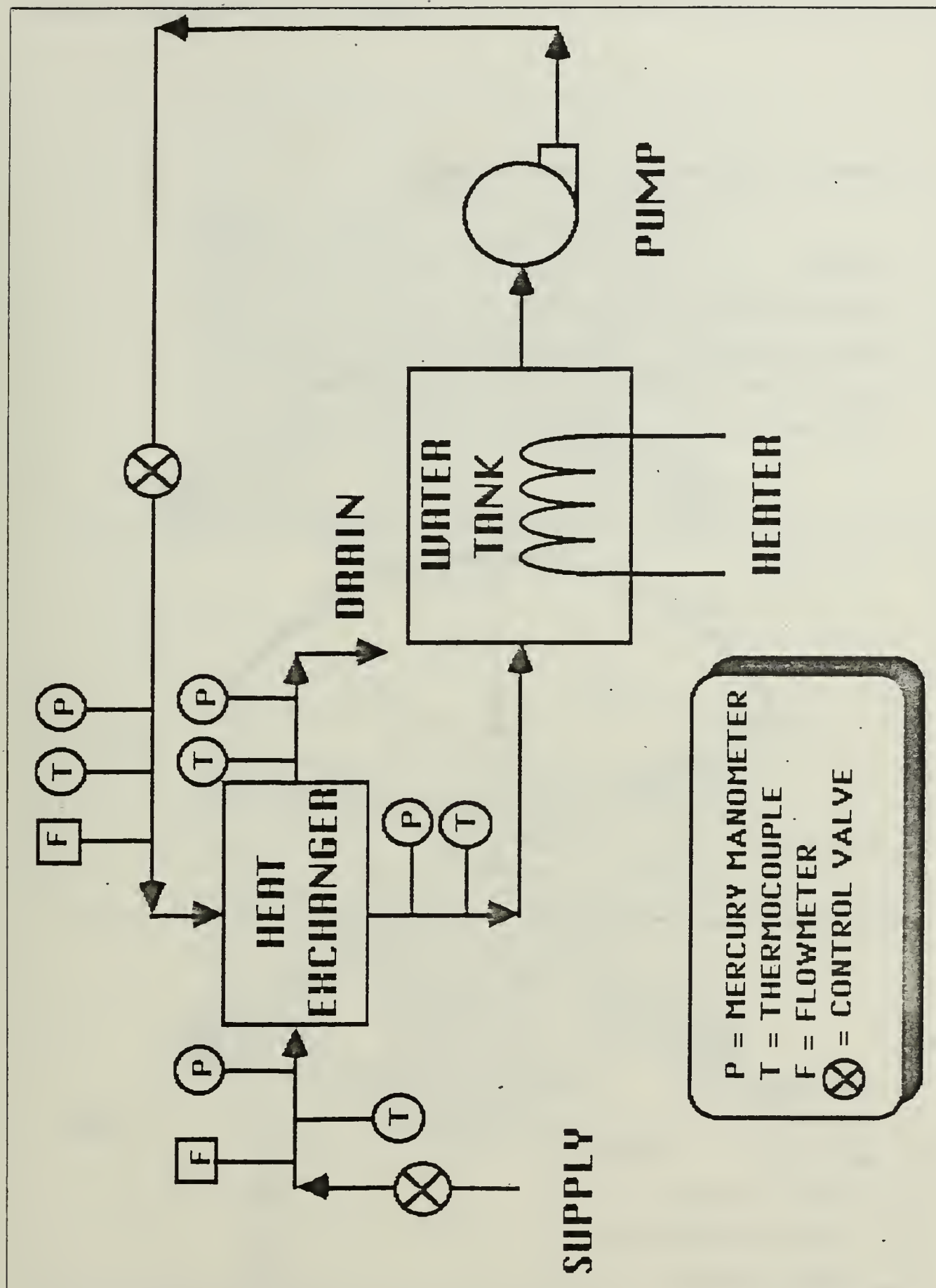


Figure 4.1 Schematic diagram of the experimental system.

2. Geometric Properties Of The Heat Exchanger

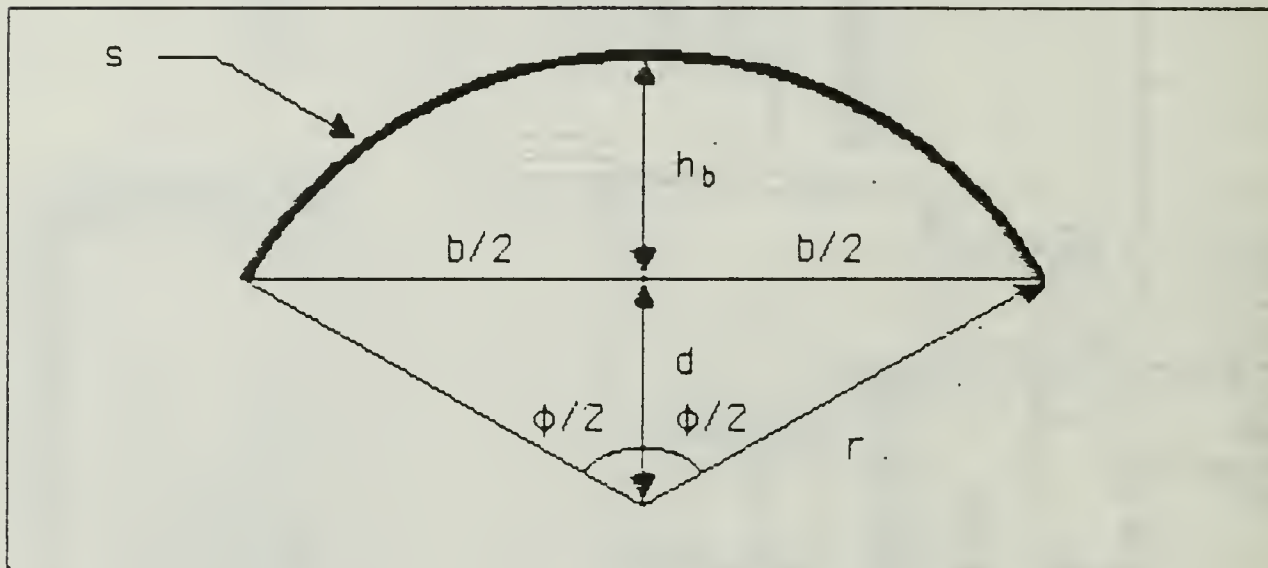
PLATE

Plate surface area : $A_s = L w$

Bump surface area : $A_{bs} = 2 \pi r h_b$

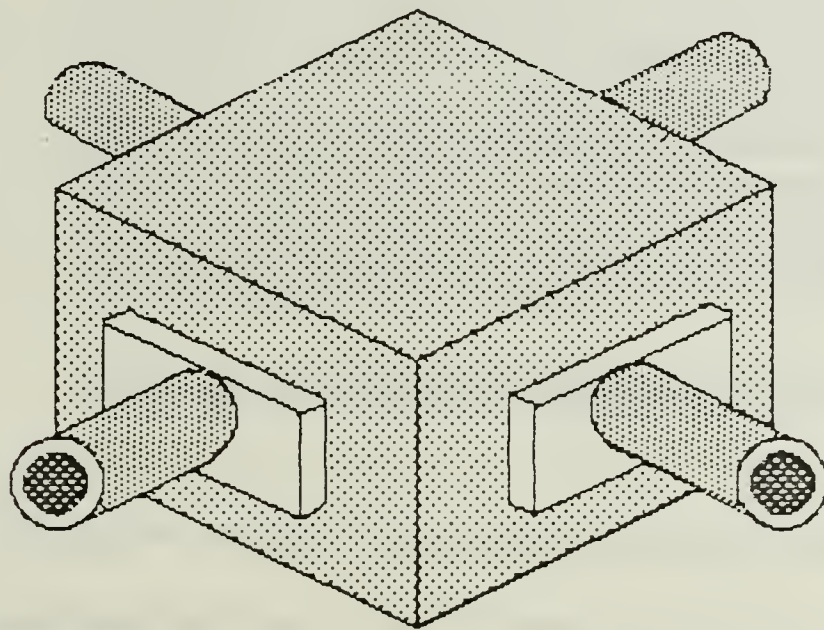
Bump cross section area : $A_{bc} = (\pi r^2 \Phi / 360) - (bd/2)$

Bump base area : $A_{bb} = \pi b^2 / 4$

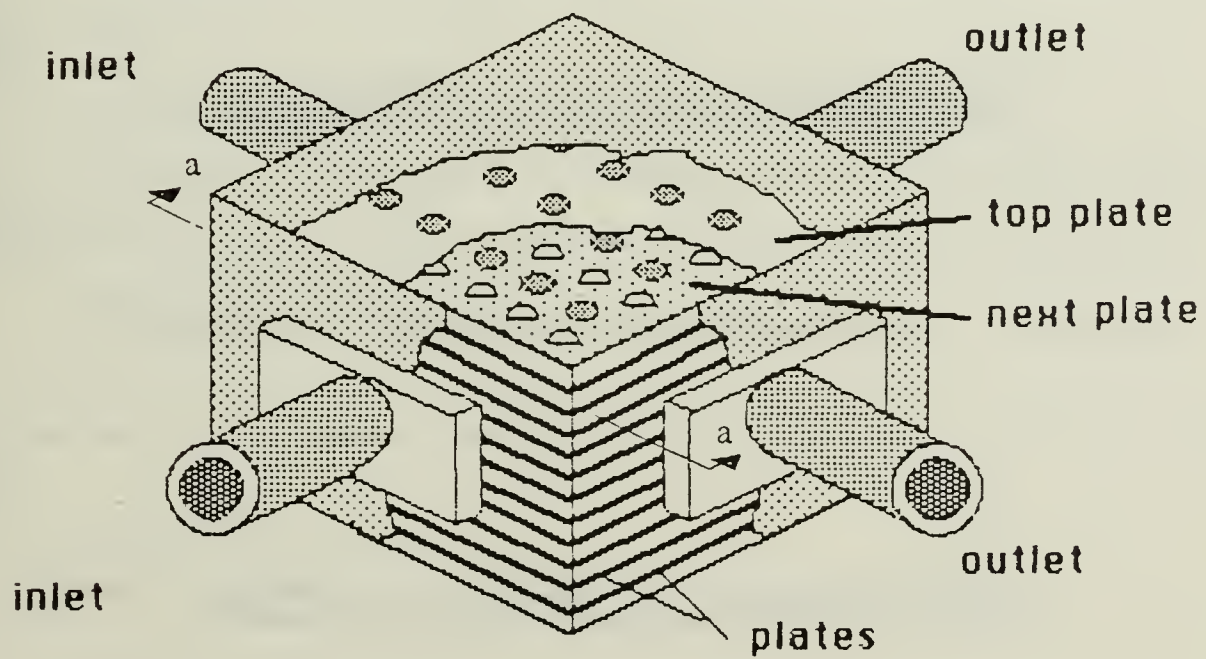


where

A_s : plate surface area	$[m^2]$
L : plate length	$[m]$
w : plate width	$[m]$
A_{bs} : bump surface area	$[m^2]$
A_{bc} : bump cross section area	$[m^2]$
A_{bb} : bump base area	$[m^2]$
h_b : bump height	$[m]$
b : bump base diameter	$[m]$



(a)



(b)

Figure 4.2 Schematic view of the heat exchanger.

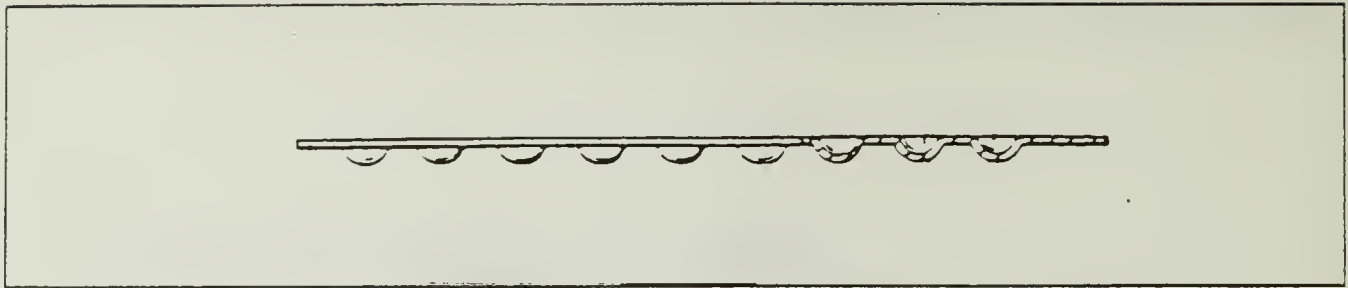


Figure 4.3 A detached edge view of the top plate configuration.

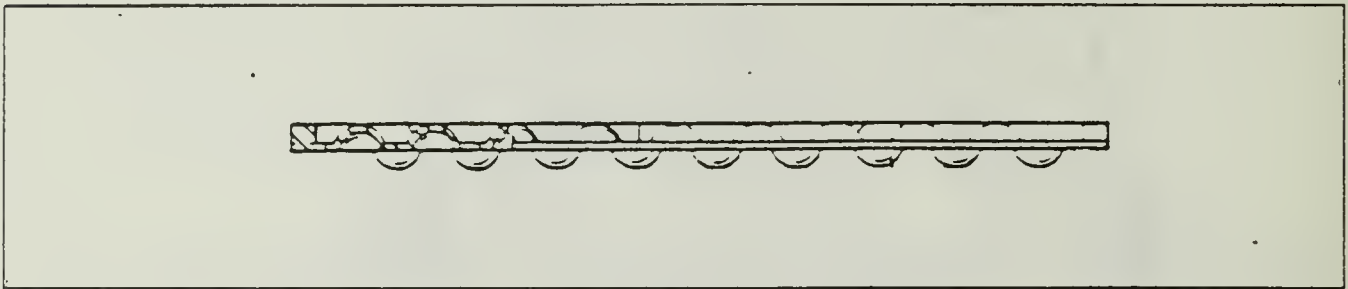


Figure 4.4 A detached edge view of another type of configuration.

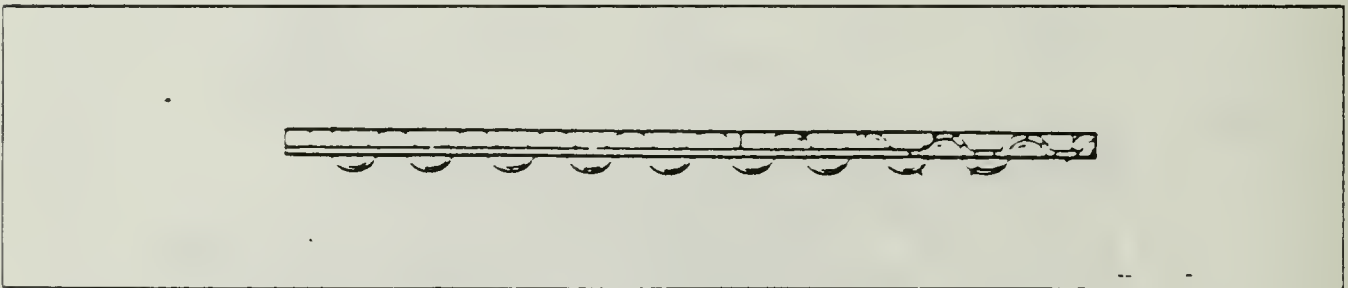


Figure 4.5 A detached edge view of another type of configuration.

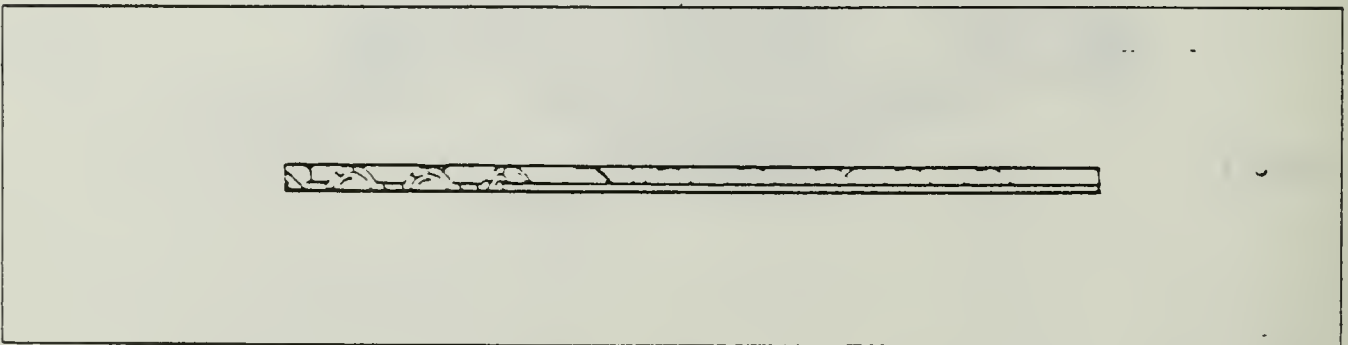


Figure 4.6 A detached edge view of the bottom plate configuration.

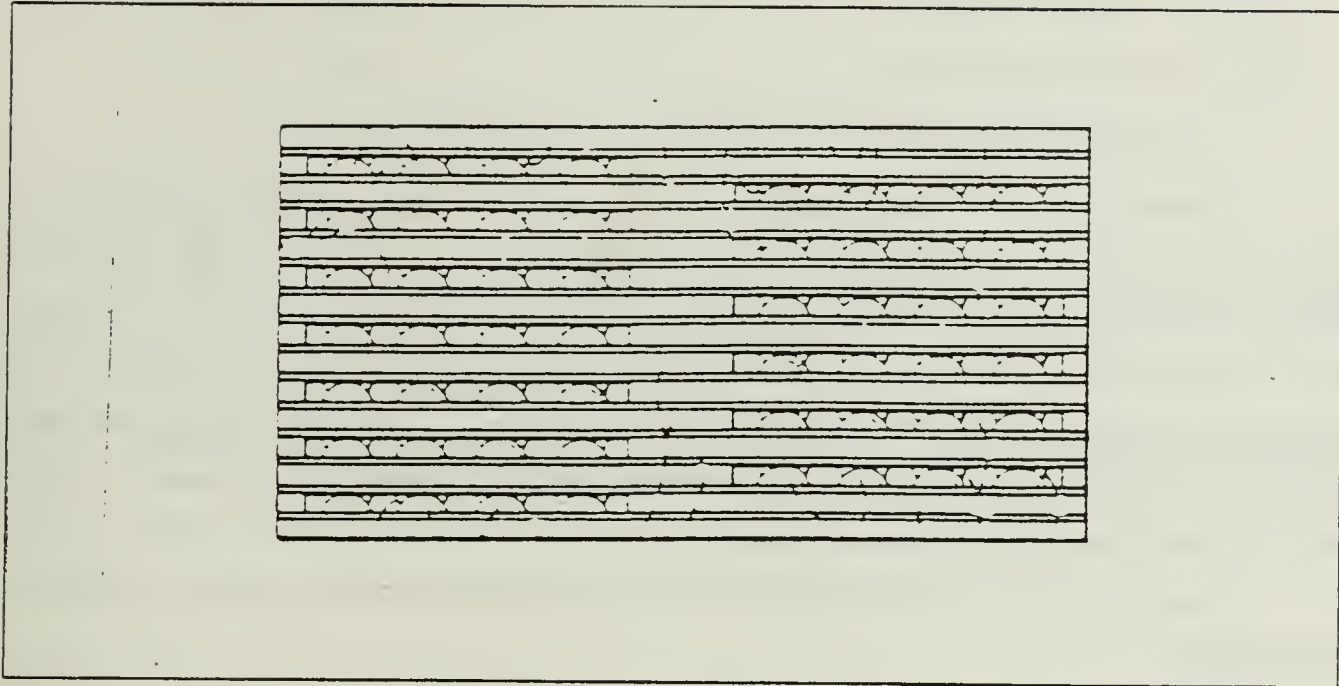


Figure 4.7 The plate configurations in the heat exchanger.

PASSAGE FLOW AREAS

$$\text{Hot passage flow area : } A_{fh} = L t_p - N_h A$$

$$\text{Cold passage flow area : } A_{fc} = w t_p - N_c A$$

where

t_p : passage height, [m]

N_h and N_c are the numbers of bumps on hot and cold sides of the plate, respectively.

EQUIVALENT DIAMETER

$$D = 4 A_f / P$$

where

A_f : passage flow area [m²]

P : wetted perimeter [m]

$$P_h = 2 L + N_h (s - b)$$

$$P_c = 2 w + N_c (s - b)$$

where

s : arc length of the bump [m]

b : bump base diameter [m]

P_h : hot wetted perimeter [m]

P_c : cold wetted perimeter [m]

3. Instrumentation

Temperature measurements were made using Copper-Constantan thermocouples using a distilled water-ice bath reference. A total of 16 thermocouples were used with individual selection being made with a thermocouple selector switch. This switch and an individual connector plug were installed in a tightly closed, insulated metal box to keep all the connecting junctions at a uniform temperature and thus reduce errors from connecting junctions. Four thermocouples were used on each inlet and outlet section of the heat exchanger.

Pressure drops across the heat exchanger were measured using two mercury manometers.

Other instrumentation included digital flow-meters used to measure and control mass flow-rate so that a steady-state condition was assured.

V. CONCLUSIONS AND RECOMMENDATIONS

A. CONCLUSIONS

The effects on the convective heat transfer coefficient of protuberances has been investigated in the fully-developed, laminar flow regime.

The effects of protuberances are beneficial as they :

1. Increase the structural rigidity which permits the use of thinner plate material and further enhances the heat transfer characteristics.
2. Create turbulence which augments the heat transfer characteristics.

The heat transfer correlations obtained are as follows :

$$Nu = 0.113 Re^{.62} Pr^{1/3} (\mu/\mu_w)^{.14}$$

$$j = 0.109 Re^{-.38} (\mu/\mu_w)^{.14}$$

$$f = 0.549 Re^{-.40} (\mu/\mu_w)^{-.14}$$

B. RECOMMENDATIONS

The present study has been associated with the laminar flow regime. Additional testing should be carried out in the turbulent flow regime.

A data acquisition system should be employed in future testing to improve accuracy.

APPENDIX A

SAMPLE CALCULATIONS

1. CONSTANT VALUES

Heat exchanger overall dimensions :

length	209.55mm	(8.25in)
width	205.58mm	(8.094in)
height	63.5mm	(2.5in)
Plate length	108.74mm	(4.28125in)
Plate width	104.78mm	(4.125in)
Plate area	11393.8mm ²	(17.66in ²)
Bump surface area	108.7mm ²	(0.16855in ²)
Bump cross sectional area	226mm ²	(0.3503in ²)
Bump base area	77.1mm ²	(0.1195in ²)
Effective heat transfer area (per plate)	14243.9mm ²	(27.078in ²)
Total effective heat transfer area (one side)	199414.2mm ²	(309.092in ²)
Hot passage flow area	141.9mm ²	(0.21989in ²)
Cold passage flow area	106.7mm ²	(0.1653in ²)
Hot side equivalent diameter	2.36mm.	(0.093in)
Cold side equivalent diameter	1.82mm.	(0.07155in)
Flow passage height	3.175mm.	(0.125in)
Bump arc length	12.426mm.	(0.489in)
Bump arc radius	5.45mm.	(0.215in)
Bump base diameter	9.906mm.	(0.39in)
Hot wetted perimeter	240.182mm.	(9.456in)
Cold wetted perimeter	234.752mm.	(9.242in)
Bump numbers on the hot side	9	
Bump numbers on the cold side	10	

2. SAMPLE CALCULATIONS

In this thesis, the following calculation procedure was used to calculate heat transfer characteristics and to obtain the correlations.

a. CALCULATION PROCEDURE

1. Determine the bulk temperatures, T_b and t_c ,

$$T_b = (T_1 + T_2) / 2$$

and

$$t_c = (t_1 + t_2) / 2$$

2. Determine μ , C_p , ρ and k and the Capacity rates, C_c and C_h ,

$$C_c = m_c C_{pc}$$

and

$$C_h = m_h C_{ph}$$

3. Determine the exchanger effectiveness, ε ,

$$\varepsilon = C_h (T_1 - T_2) / C_{\min} (T_1 - t_1) \quad \text{if } C_h < C_c$$

or

$$\varepsilon = C_c (t_2 - t_1) / C_{\min} (T_1 - t_1) \quad \text{if } C_c < C_h$$

4. Determine the number of transfer units, N_{tu} , from ε - N_{tu} relations, both fluids unmixed, (Ref.6.)

$$\varepsilon = 1 - \exp[(1/C_r)(N_{tu})^{0.22}[\exp(-C_r(N_{tu})^{0.78}) - 1]]$$

where C_r is the capacity rate ratio, C_{\min}/C_{\max} .

5. The overall heat transfer coefficient, U , is formed from the number of transfer units.

$$U = N_{tu} C_{\min} / A$$

where A is the total effective heat transfer area.

6. The convective heat transfer coefficient, h_h , will be

$$h_h = [(1/U) - (1/h_c) - r_w]^{-1}$$

Where h_h is the hot fluid heat transfer coefficient

h_c is the cold fluid heat transfer coefficient

r_w is the wall resistance

7. The fluid velocity, V , is for either fluid

$$V = m / \rho A_f$$

where A_f is the passage flow area.

8. The wall temperature, T_w , is computed from

$$T_w = \bar{t} + [h_h / (h_h + h_c)](\bar{T} - \bar{t})$$

where \bar{T} is the average temperature of the hot fluid.

\bar{t} is the average temperature of the cold fluid.

10. Form the Prandtl number,

$$C_p \mu / k$$

the Reynolds number,

$$\rho V D / \mu$$

and the viscosity correction factor,

$$\mu / \mu_w$$

with μ_w calculated at wall temperature.

11. The friction factor, f , is determined from

$$f = (A_c v_m / A v_1) [(2 g_c \Delta T / G^2 v_1) + (1 - \sigma^2 - K_e)(v_2 / v_1) - (K_c + 1 - \sigma^2) - 2(v_2 / v_1 - 1)]$$

where v_m : fluid specific volume at mean condition.

v_1 : fluid specific volume at inlet condition.

v_2 : fluid specific volume at outlet condition.

G : mass velocity.

A : total heat transfer area.

A_f : free flow area.

σ : ratio of free-flow area to frontal area.

$\sigma_h = 0.028$ for hot side. (Ref. 6.)

$\sigma_c = 0.0178$ for cold side. (Ref. 6.)

K_c : contraction loss coefficient.

$K_c = 1.3$ both hot and cold side. (Ref. 6.)

K_e : expansion loss coefficient.

$K_{eh} = 0.92$ for hot side. (Ref. 6.)

$K_{ec} = 0.97$ for cold side. (Ref. 6.)

b. HOT WATER-COLD WATER STUDY

The experimental data is tabulated in Table 1.

The experiment results are tabulated in Tables 2, 3 and 4.

c. HOT GLYCOL-COLD WATER STUDY

The experimental data is tabulated in Table 5.

The experimental results are tabulated in Tables 6, 7 and 8.

d. HOT WATER-COLD AIR STUDY

The experimental data is tabulated in Table 9.

The experimental results are tabulated in Tables 10 and 11.

e. CALCULATION OF CORRELATIONS

1. THE CORRELATION FOR THE NUSSELT NUMBER :

All of the experimental data for a correlation for the Nusselt number are plotted in Figure A.1. Observe that the results show very little scatter, because of this, one may take runs 5 and 8 in the water-water study and begin with a proposed form :

$$Nu = C Re^m Pr^n (\mu/\mu_w)^{.14}$$

Then, it is only a matter of algebra to show that

$$\text{Log}Nu = \text{Log}C + m\text{Log}Re + n\text{Log}Pr + 0.14\text{Log}(\mu/\mu_w)$$

and from the Table 4, for runs 5 and 8 respectively

$$\text{Log}(10.2) = \text{Log}C + m\text{Log}(631.8) + (1/3)\text{Log}(4.79) + 0.14\text{Log}(0.892)$$

$$\text{Log}(11.4) = \text{Log}C + m\text{Log}(756.4) + (1/3)\text{Log}(4.80) + 0.14\text{Log}(0.887)$$

from which one may solve for C and m ,

$$C = 0.113$$

$$m = 0.62$$

Hence, the correlation is

$$Nu = 0.113 Re^{.62} Pr^{1/3} (\mu/\mu_w)^{.14}$$

2. THE CORRELATION FOR THE COLBURN FACTOR :

All of the experimental data for a correlation for the Colburn factor are plotted in Figure A.2. Observe that the results show very little scatter. Because of this, one may take runs 5 and 15 in the glycol-water study and begin with a proposed form :

$$j = C Re^m (\mu/\mu_w)^{.14} \text{ and}$$

$$\text{Log} j = \text{Log} C + m \text{Log} Re + 0.14 \text{Log}(\mu/\mu_w)$$

and from the Table 8, for runs 5 and 15 respectively

$$\text{Log}(0.0258) = \text{Log} C + m \text{Log}(42.77) + 0.14 \text{Log}(0.651)$$

$$\text{Log}(0.0200) = \text{Log} C + m \text{Log}(83.15) + 0.14 \text{Log}(0.652)$$

from which one may solve for C and m,

$$C = 0.109$$

$$m = - 0.38$$

Hence, the correlation is

$$j = St Pr^{2/3} (\mu/\mu_w)^{.14}$$

$$j = 0.109 Re^{-.38} (\mu/\mu_w)^{.14}$$

where St is the Stanton number, $St = h/\rho C_p V$.

3. THE CORRELATION FOR THE FRICTION FACTOR :

All of the experimental data for a correlation for the friction factor are plotted in Figure A.3. Observe that the results show very little scatter. Because of this, one may take runs 2 and 18 in the water-water study and begin with a proposed form :

$$f = C Re^m (\mu/\mu_w)^{-.14} \text{ and}$$

$$\text{Log} f = \text{Log} C + m \text{Log} Re - 0.14 \text{Log}(\mu/\mu_w)$$

and from the Table 11, for runs 2 and 18 respectively

$$\text{Log}(0.051) = \text{Log}C + m\text{Log}(378.4) - 0.14\text{Log}(0.896)$$

$$\text{Log}(0.031) = \text{Log}C + m\text{Log}(1301.0) - 0.14\text{Log}(0.897)$$

from which one may solve for C and m ,

$$C = 0.549$$

$$m = -0.40$$

Hence, the correlation is

$$f = 0.549 \text{ Re}^{-.40} (\mu/\mu_w)^{-.14}$$

TABLE 1
THE EXPERIMENTAL DATA FOR THE WATER-WATER STUDY

RUN NO	ΔP in H_2O	m_h	m_c	HOT WATER		COLD WATER	
				T_1	T_2	t_1	t_2
1	1.36	0.089	0.089	37.38	33.06	21.90	26.22
2	2.04	0.114	0.114	37.40	33.42	22.82	26.80
3	3.13	0.146	0.146	37.30	33.71	22.94	26.53
4	4.08	0.171	0.171	37.28	33.72	22.87	26.43
5	4.76	0.190	0.190	37.25	33.73	22.70	26.22
6	5.44	0.206	0.206	37.15	33.66	22.55	26.04
7	5.71	0.216	0.216	37.20	33.75	22.39	25.84
8	6.12	0.229	0.229	37.10	33.67	22.12	25.55
9	7.48	0.248	0.248	36.90	33.52	21.88	25.26
10	8.16	0.267	0.267	36.80	33.48	21.85	25.17
11	9.65	0.286	0.286	36.10	32.96	21.70	24.84
12	10.47	0.305	0.305	35.90	32.77	21.41	24.54
13	12.24	0.330	0.330	35.50	32.44	21.23	24.29
14	13.32	0.349	0.349	35.30	32.30	21.15	24.15
15	13.60	0.368	0.368	35.00	32.13	21.18	24.06
16	15.64	0.381	0.381	34.60	31.80	20.81	23.61
17	16.32	0.400	0.400	34.50	31.75	20.88	23.63
18	17.68	0.412	0.412	34.35	31.68	21.00	23.67

TABLE 2
PROPERTIES OF THE HOT WATER

RUN NO	T _{bh}	ρ	C _p	$\mu \cdot 10^6$	k 10^3
1	35.22	1006.30	4178	721.344	625.152
2	35.41	1006.40	4178	718.532	625.456
3	35.51	1006.40	4178	717.126	625.608
4	35.50	1006.40	4178	717.200	625.600
5	35.49	1006.40	4178	717.348	625.584
6	35.41	1006.36	4178	718.606	625.448
7	35.48	1006.40	4178	717.570	625.560
8	35.39	1006.35	4178	718.902	625.416
9	35.21	1006.30	4178	721.492	625.136
10	35.14	1006.26	4178	722.528	625.024
11	34.53	1006.01	4178	731.556	624.048
12	34.34	1005.90	4178	734.442	623.736
13	33.97	1005.80	4178	739.844	623.152
14	33.80	1005.70	4178	742.360	622.880
15	33.56	1005.60	4178	745.875	622.500
16	33.20	1005.50	4178	751.240	621.920
17	33.13	1005.40	4178	752.350	621.800
18	33.02	1005.40	4178	753.980	621.624

TABLE 3
SOME RESULTS OF THE WATER-WATER STUDY

RUN NO	ϵ	N_{tu}	U	h_h	h_c	T_w
1	0.279	0.396	737.40	1510.2	1510.2	29.64
2	0.273	0.384	919.48	1894.2	1894.2	30.11
3	0.250	0.339	1037.25	2145.0	2145.0	30.12
4	0.247	0.334	1199.68	2494.2	2494.2	30.08
5	0.242	0.324	1293.06	2696.7	2696.7	29.98
6	0.239	0.319	1379.15	2884.4	2884.4	29.85
7	0.233	0.308	1393.09	2914.9	2914.9	29.80
8	0.229	0.301	1441.46	3021.0	3021.0	29.61
9	0.225	0.294	1525.16	3205.3	3205.3	29.39
10	0.222	0.289	1613.16	3400.2	3400.2	29.32
11	0.218	0.282	1687.52	3565.8	3565.8	28.90
12	0.216	0.279	1780.73	3774.5	3774.5	28.50
13	0.214	0.276	1903.12	4050.6	4050.6	28.36
14	0.212	0.272	1988.80	4245.3	4245.3	28.23
15	0.208	0.266	2050.83	4386.9	4386.9	28.10
16	0.203	0.257	2049.47	4425.1	4425.1	27.70
17	0.202	0.256	2143.50	4599.6	4599.6	27.69
18	0.200	0.253	2185.54	4696.6	4696.6	27.68

TABLE 4
SOME RESULTS OF THE WATER-WATER STUDY

RUN NO	Nu	Pr	St	Re	μ/μ_w	f	j
1	5.7	4.82	0.0040	293.3	0.891	0.055	0.0115
2	7.2	4.80	0.0039	378.4	0.896	0.051	0.0112
3	8.1	4.79	0.0035	484.5	0.896	0.049	0.0099
4	9.4	4.79	0.0035	568.7	0.894	0.048	0.0098
5	10.2	4.79	0.0034	631.8	0.892	0.043	0.0095
6	10.9	4.80	0.0033	683.2	0.892	0.042	0.0094
7	11.0	4.79	0.0032	715.7	0.889	0.041	0.0091
8	11.4	4.80	0.0031	756.4	0.887	0.040	0.0089
9	12.1	4.82	0.0031	816.5	0.886	0.040	0.0088
10	12.9	4.90	0.0030	878.0	0.886	0.039	0.0087
11	13.5	4.92	0.0030	928.9	0.890	0.040	0.0086
12	14.3	4.96	0.0029	986.8	0.889	0.038	0.0085
13	15.4	4.98	0.0029	1061.1	0.890	0.038	0.0085
14	16.1	5.01	0.0029	1118.3	0.891	0.037	0.0084
15	16.7	5.05	0.0028	1173.8	0.892	0.036	0.0083
16	16.8	5.06	0.0028	1205.4	0.891	0.034	0.0081
17	17.5	5.07	0.0027	1262.9	0.894	0.033	0.0081
18	17.9	5.12	0.0027	1301.0	0.897	0.031	0.0080

TABLE 5
THE EXPERIMENTAL DATA FOR THE GLYCOL-WATER STUDY

RUN NO	ΔP inHg	m_h	m_c	HOT GLYCOL		COLD WATER	
				T_1	T_2	t_1	t_2
1	0.3	0.098	0.089	36.5	33.73	21.0	22.8
2	0.4	0.125	0.114	36.5	33.80	21.0	22.7
3	0.5	0.160	0.146	36.5	33.97	21.0	22.6
4	0.6	0.188	0.171	36.4	33.93	21.0	22.6
5	0.8	0.209	0.190	36.4	33.99	21.0	22.6
6	0.9	0.227	0.206	36.4	34.03	20.9	22.4
7	1.0	0.237	0.216	36.4	34.09	20.9	22.4
8	1.1	0.251	0.229	36.5	34.24	20.9	22.4
9	1.3	0.272	0.248	36.5	34.30	21.0	22.4
10	1.4	0.293	0.267	36.5	34.33	21.0	22.4
11	1.6	0.314	0.286	36.5	34.37	21.0	22.4
12	1.8	0.335	0.305	36.5	34.44	21.0	22.3
13	2.1	0.363	0.330	36.5	34.47	21.0	22.3
14	2.3	0.383	0.349	36.5	34.50	21.0	22.3
15	2.6	0.404	0.368	36.5	34.53	21.0	22.3
16	2.7	0.418	0.381	36.4	34.46	20.9	22.1
17	2.9	0.439	0.400	36.4	34.50	20.9	22.1
18	3.1	0.453	0.412	36.4	34.53	20.9	22.1

TABLE 6
PROPERTIES OF THE HOT GLYCOL

RUN NO	T _{bh}	ρ	C _p	$\mu \cdot 10^2$	k 10^3
1	35.12	1109.94	2452	1.164	254.5
2	35.15	1104.91	2452	1.163	254.5
3	35.24	1104.96	2452	1.158	254.5
4	35.17	1104.94	2452	1.162	254.5
5	35.20	1104.92	2452	1.160	254.5
6	35.22	1105.05	2452	1.159	254.5
7	35.25	1105.02	2452	1.158	254.5
8	35.37	1105.01	2452	1.152	254.5
9	35.40	1105.03	2452	1.150	254.5
10	35.42	1105.05	2452	1.149	254.5
11	35.44	1105.02	2452	1.148	254.5
12	35.47	1104.96	2452	1.147	254.5
13	35.49	1105.03	2452	1.146	254.5
14	35.50	1105.05	2452	1.145	254.5
15	35.52	1105.05	2452	1.144	254.5
16	35.43	1104.96	2452	1.149	254.5
17	35.45	1105.00	2452	1.148	254.5
18	35.47	1104.96	2452	1.147	254.5

TABLE 7
SOME RESULTS OF THE GLYCOL-WATER STUDY

RUN NO	ε	N_{tu}	U	h_h	h_c	T_w
1	0.179	0.210	270.01	332.30	1510.2	24.77
2	0.174	0.204	314.73	382.02	1894.2	24.74
3	0.163	0.189	372.64	457.53	2145.0	25.00
4	0.160	0.185	428.15	525.49	2494.2	24.95
5	0.156	0.180	462.88	568.88	2696.7	24.86
6	0.153	0.176	490.38	602.11	2884.4	24.83
7	0.149	0.170	495.55	608.56	2914.9	24.98
8	0.145	0.165	509.23	624.59	3021.0	24.99
9	0.142	0.161	538.30	660.49	3205.3	24.99
10	0.140	0.159	572.51	703.79	3400.2	24.89
11	0.137	0.155	597.99	735.23	3565.8	24.86
12	0.133	0.150	617.24	755.59	3774.5	24.81
13	0.131	0.147	655.32	801.67	4050.6	24.66
14	0.129	0.145	683.71	836.57	4245.3	24.65
15	0.127	0.142	706.09	864.60	4386.9	24.72
16	0.125	0.140	720.08	884.13	4425.1	24.74
17	0.123	0.137	739.89	907.08	4599.6	24.60
18	0.121	0.135	752.25	921.90	4696.6	24.55

TABLE 8
SOME RESULTS OF THE GLYCOL-WATER STUDY

RUN NO	Nu	Pr	St	Re	μ/μ_w	f	j
1	3.1	112.18	0.00130	21.37	0.650	0.142	0.0302
2	4.0	112.01	0.00125	25.69	0.651	0.115	0.0290
3	4.2	111.89	0.00116	32.85	0.653	0.090	0.0270
4	4.9	112.25	0.00114	38.45	0.654	0.090	0.0266
5	5.3	112.11	0.00111	42.77	0.651	0.094	0.0258
6	5.6	111.54	0.00108	46.57	0.651	0.090	0.0249
7	5.7	111.37	0.00104	48.80	0.655	0.090	0.0241
8	5.8	111.68	0.00101	51.52	0.653	0.090	0.0234
9	6.1	111.58	0.00098	55.86	0.653	0.087	0.0228
10	6.5	111.52	0.00098	60.19	0.656	0.084	0.0226
11	6.8	111.42	0.00095	64.55	0.656	0.082	0.0220
12	7.0	111.68	0.00092	68.70	0.655	0.081	0.0213
13	7.4	111.61	0.00089	74.47	0.649	0.080	0.0207
14	7.8	111.54	0.00088	78.82	0.650	0.080	0.0205
15	8.0	111.49	0.00087	83.15	0.652	0.080	0.0200
16	8.2	111.89	0.00086	85.71	0.656	0.079	0.0200
17	8.4	111.82	0.00084	90.05	0.647	0.077	0.0195
18	8.6	111.75	0.00083	92.97	0.647	0.077	0.0193

TABLE 9
THE EXPERIMENTAL DATA FOR THE WATER-AIR STUDY

RUN NO	ΔP in H_2O	m_h	$m_c \cdot 10^3$	HOT WATER		COLD AIR	
				T_1	T_2	t_1	t_2
1	1.2	0.190	1.91	36.8	36.8	19.6	36.5
2	2.5	0.190	2.87	36.8	36.7	19.6	36.3
3	4.0	0.190	3.83	36.8	36.7	19.6	36.0
4	6.0	0.190	4.79	36.9	36.8	19.6	36.9
5	8.0	0.190	5.75	36.9	36.8	19.6	35.8
6	10.8	0.190	6.70	36.9	36.8	19.8	35.6
7	13.7	0.190	7.66	36.9	36.7	19.8	35.5
8	17.0	0.190	8.62	36.9	36.7	19.8	35.3
9	19.3	0.190	9.58	37.0	36.8	19.9	35.3

TABLE 10
SOME RESULTS OF THE WATER-AIR STUDY

RUN NO	ε	N_{tu}	U	h_h	h_c
1	0.983	4.12	39.74	2696.7	40.58
2	0.971	3.58	51.88	2696.7	52.99
3	0.953	3.09	59.76	2696.7	61.23
4	0.942	2.88	69.66	2696.7	71.67
5	0.936	2.78	80.72	2696.7	83.43
6	0.924	2.61	88.31	2696.7	91.56
7	0.918	2.53	97.86	2696.7	101.88
8	0.906	2.40	104.47	2696.7	109.06
9	0.901	2.35	113.69	2696.7	119.14

TABLE 11
SOME RESULTS OF THE WATER-AIR STUDY

RUN NO	Nu	Pr	St	Re	f	j
1	2.8	0.707	0.0156	251.8	0.055	0.0124
2	3.7	0.707	0.0136	378.4	0.051	0.0108
3	4.2	0.707	0.0118	504.9	0.046	0.0094
4	5.0	0.707	0.0111	631.5	0.044	0.0088
5	5.8	0.707	0.0108	758.0	0.040	0.0086
6	6.3	0.707	0.0101	883.3	0.040	0.0080
7	7.0	0.707	0.0098	1009.8	0.039	0.0078
8	7.5	0.707	0.0093	1136.4	0.038	0.0074
9	8.2	0.707	0.0092	1263.0	0.035	0.0073

A CORRELATION FOR NU

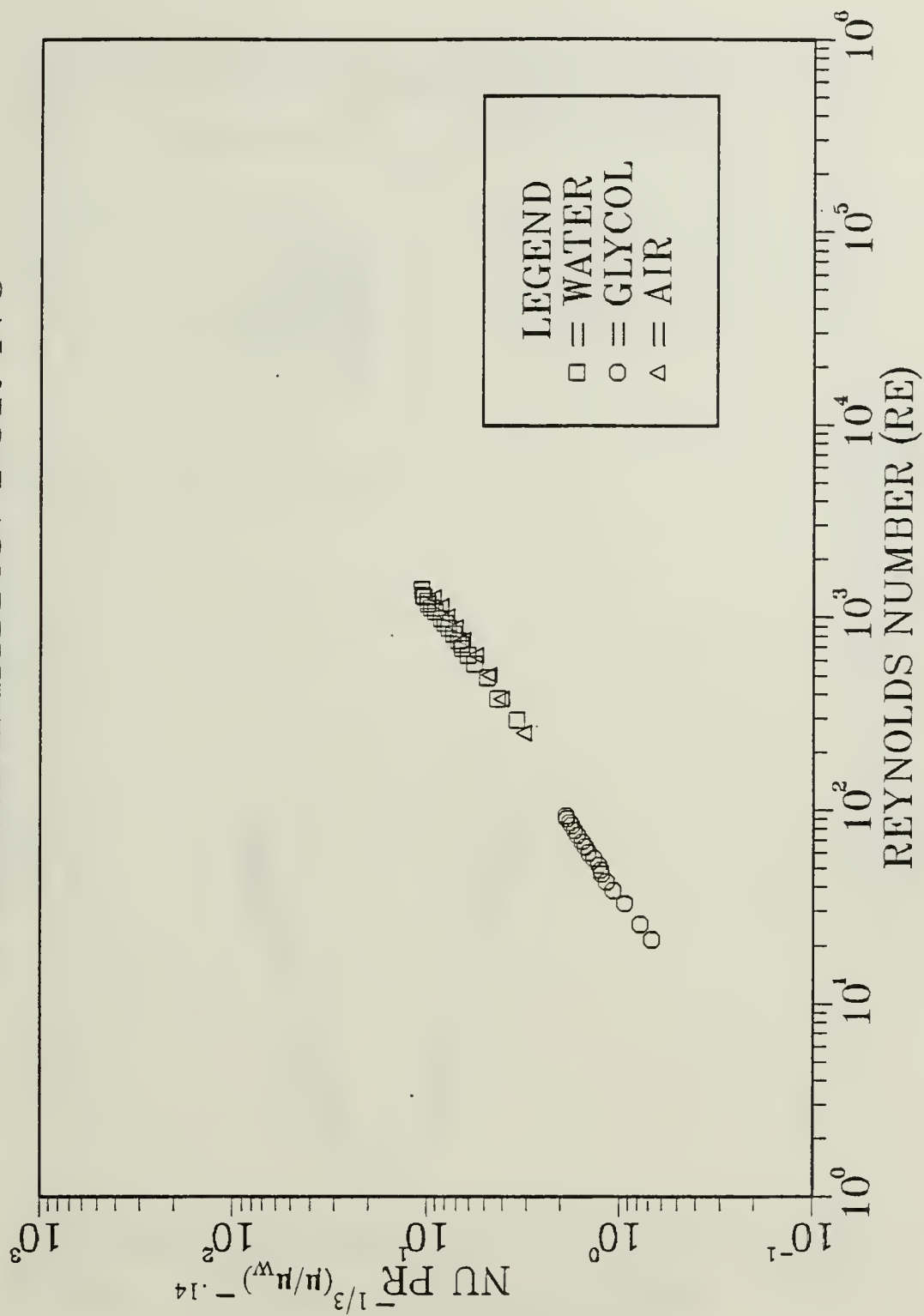


Figure A.1 A correlation for the Nusselt number.

A CORRELATION FOR J

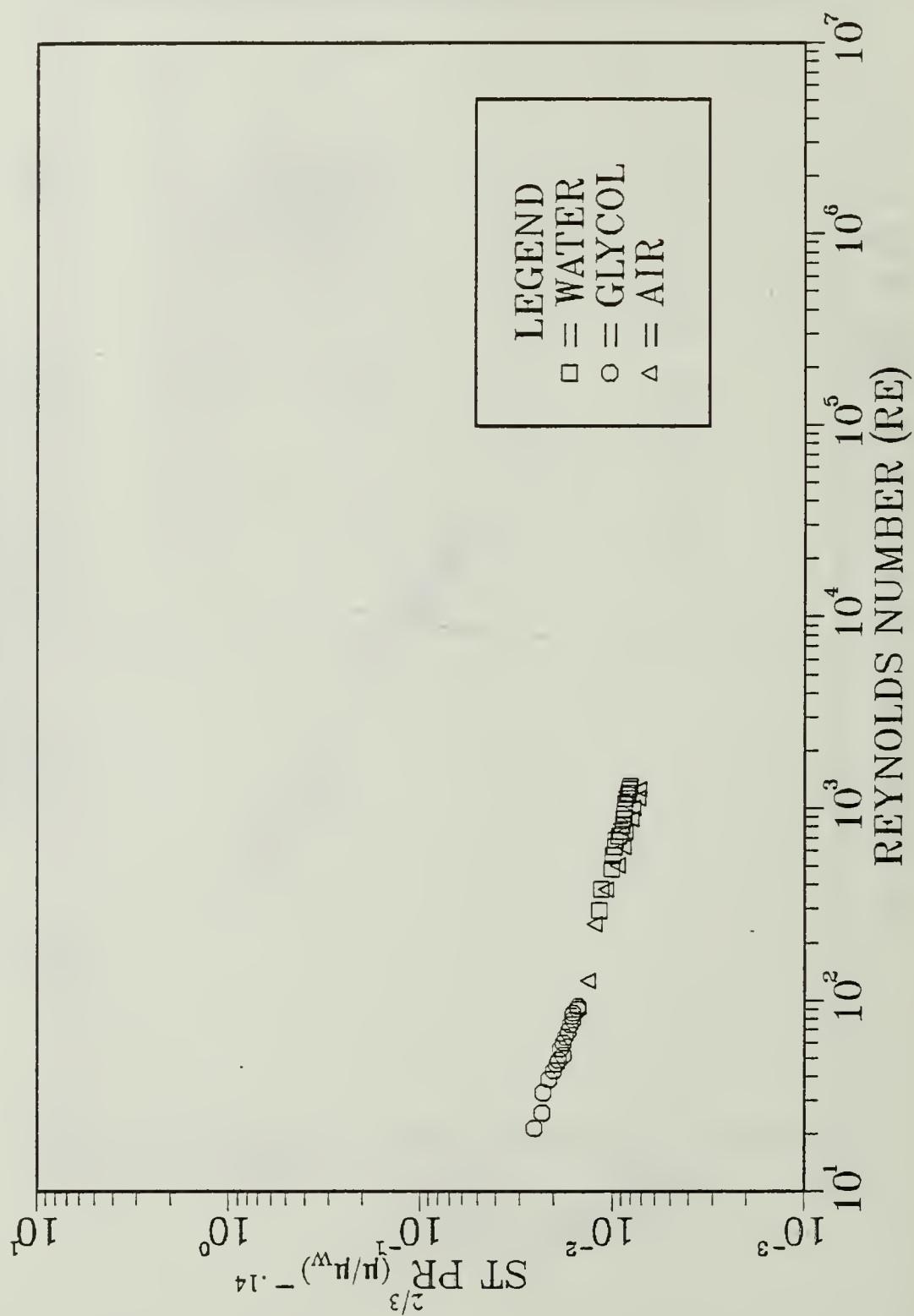


Figure A.2 A correlation for the Colburn factor.

A CORRELATION FOR F

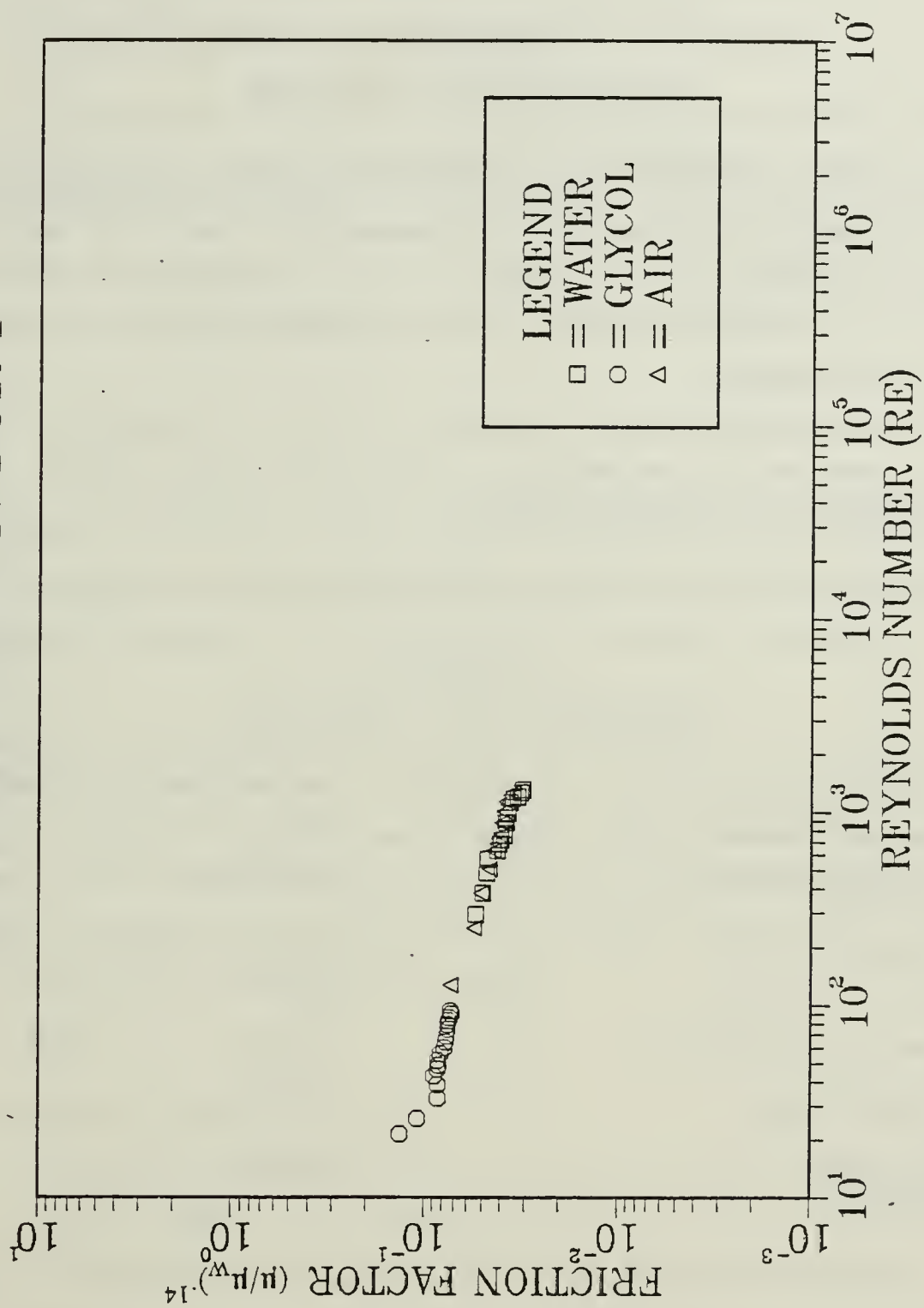


Figure A.3 A correlation for the friction factor.

APPENDIX B

DIMENSIONAL ANALYSIS

The dependent variable for the process is the convection heat transfer coefficient, h . For incompressible low-speed flow the independent variables that determine the heat transfer coefficient are the fluid velocity, V , a linear dimension (e.g., the equivalent diameter, D), and the fluid properties of thermal conductivity, k , viscosity, μ , specific heat, C_p , and density ρ .

The independent dimensional quantities to be used in the analysis are mass, M ; length, L ; time, Θ ; and temperature, T . The variables, their symbols, and their dimensional equations are listed in Table 12.

TABLE 12
VARIABLES FOR CONVECTION

VARIABLE	SYMBOL	DIMENSIONAL EQUATION
Equivalent diameter	D	$[L]$
Thermal conductivity of the fluid	k	$[ML/\Theta^3T]$
Velocity of the fluid	V	$[L/\Theta]$
Density of the fluid	ρ	$[M/L^3]$
Viscosity of the fluid	μ	$[M/L\Theta]$
Specific heat at constant pressure	C_p	$[L^2/\Theta^2T]$
Heat transfer coefficient	h	$[M/\Theta^3T]$

There are seven physical quantities and four primary dimensions. We therefore expect that three dimensionless groups will be required to correlate experimental data. To determine these dimensionless groups, write as a product of each of the variables raised to an unknown power:

$$\Pi = D^a k^b v^c \rho^d \mu^e C_p^f h^g$$

and then substitute the dimensional formulas from the tabulation above:

$$\Pi = [L]^a [ML/\Theta^3 T]^b [L/\Theta]^c [M/L^3]^d [M/L\Theta]^e [L^2/\Theta^2 T]^f [M/\Theta^3 T]^g$$

For Π to be dimensionless, the exponents of each primary dimension must separately add to zero. Equating the sum of the exponents of each primary dimension to zero yields the following set of equations:

$$\begin{aligned} b + d + e + g &= 0 && \text{for } M \\ a + b + c - 3d - e + 2f &= 0 && \text{for } L \\ -3b - c - e - 2f - 3g &= 0 && \text{for } \Theta \\ -b - f - g &= 0 && \text{for } T \end{aligned}$$

Since there are seven unknowns but only four equations, three of the exponents can be arbitrarily selected for each dimensionless group. The only restriction is that each of the arbitrarily selected exponents be independent of the other. This requirement is met if the determinant formed by the coefficients of the remaining terms does not equal zero.

Since the convection heat transfer coefficient is the dependent variable that we eventually want to evaluate, set its exponent g equal to unity in the first dimensionless group, Π_1 . To simplify the algebraic manipulations, arbitrarily set $c = d = 0$. This means that in the first dimensionless group velocity and density will not appear.

Solving the equations above simultaneously, we obtain $a = 1$, $b = -1$, and $e = f = 0$. The first dimensionless group is therefore

$$\Pi_1 = hD/k$$

which we recognize as the Nusselt number.

For the second dimensionless group, we set $g = 0$ to avoid having the dependent variable h appear again. Arbitrarily, we let $a = 1$ and $f = 0$. Simultaneous solution of the equations above with these choices yields the second parameter,

$$\Pi_2 = VD\rho/\mu$$

which we recognize as the Reynolds number, Re .

For the third dimensionless group, we wish to have the specific heat, which has not appeared in any previous group, to be included and therefore set $f = 1$. Similarly, we do not wish to have the heat transfer coefficient or the diameter appear again and therefore let a and g equal to 0. This yields the third dimensionless group,

$$\Pi_3 = C_p \mu / k$$

which we recognize as the Prandtl number, Pr . Thus the heat transfer coefficient in Π_1 can be functionally related to the dimensionless groups Π_2 and Π_3 in the form

$$Nu = f(Re, Pr)$$

APPENDIX C

UNCERTAINTY ANALYSIS

The uncertainties for the major variable in the experiments were calculated in accordance with the method described by S. Kline and F. McClintoch (Ref. 9.). The estimates of the uncertainties were made conservatively. As a result, there is considerable confidence in the uncertainties as calculated.

The following equations were used to calculate the uncertainties.

1. $\partial T_b/T_b = [(\partial T_1/T_1)^2 + (\partial T_2/T_2)^2]^{1/2}$
2. $\partial C_h/C_h = [(\partial m/m)^2 + (\partial C_p/C_p)^2]^{1/2}$
3. $\partial \epsilon = [(\partial C_h/C_h)^2 + (\partial T_1/T_1)^2 + (\partial T_2/T_2)^2 + (\partial t_1/t_1)^2]^{1/2}$
4. $\partial N_{tu}/N_{tu} = [(\partial C_r/C_r)^2 + (\partial \epsilon/\epsilon)^2]^{1/2}$
5. $\partial U/U = [(\partial N_{tu}/N_{tu})^2 + (\partial C_h/C_h)^2 + (\partial A/A)^2]^{1/2}$
6. $\partial V/V = [(\partial m/m)^2 + (\partial \rho/\rho)^2 + (\partial A_f/A_f)^2]^{1/2}$
7. $\partial h/h = [(\partial U/U)^2 + (\partial r_w/r_w)^2]^{1/2}$
8. $\partial Pr/Pr = [(\partial C_p/C_p)^2 + (\partial \mu/\mu)^2 + (\partial k/k)^2]^{1/2}$
9. $\partial Re/Re = [(\partial \rho/\rho)^2 + (\partial V/V)^2 + (\partial D/D)^2 + (\partial \mu/\mu)^2]^{1/2}$
10. $\partial Nu/Nu = [(m\partial Re/Re)^2 + (n\partial Pr/Pr)^2]^{1/2}$
11. $\partial f/f = (m\partial Re/Re)$
12. $\partial j/j = (m\partial Re/Re)$

The following quantities had their uncertainty calculated by dividing the estimated error in the quantity by the value of the quantity and these uncertainties are considered constant for the range of values in this experiment.

Quantity	Uncertainty
A	0.003
A_f	0.005
D	0.006
μ	0.005
k	0.003
ρ	0.002
m	0.008
C_p	0.005
r_w	0.003

The following quantities had the worst case error

Quantity	Error
T_1	± 0.2
T_2	± 0.2
t_1	± 0.2
t_2	± 0.2
ΔT	± 0.3

Then, the uncertainties for the following quantities were calculated using the equations above,

Quantity	Uncertainty
T_b	0.008
C_h	0.01
ε	0.012
N_{tu}	0.015
U	0.018
h	0.018
V	0.01
Pr	0.009
Re	0.013
Nu	0.009

f	0.005
j	0.005

LIST OF REFERENCES

1. Incropera, F.P., and Dewitt, D.P., *Fundamentals of Heat and Mass Transfer*, John Wiley & Sons, New York, NY, 1985.
2. Shah, R.K. and London, A.L., *Laminar Flow Forced Convection in Ducts*, Academic Press, New York, NY, 1978.
3. Burmeister, L.C., *Convective Heat Transfer*, John Wiley & Sons, New York, NY, 1983.
4. Kreith, F., and Black, W.Z., *Basic Heat Transfer*, Harper & Row Publishers, New York, NY, 1980.
5. Kreith, F., *Principles of Heat Transfer, Second Edition*, International Textbook Company, Scranton, PA, 1968.
6. Kays, W.M., and London, A.L., *Compact Heat Exchangers, Third Edition*, McGraw-Hill Book Company, New York, NY, 1985.
7. Kern, D.Q. and Kraus, A.D., *Extended Surface Heat Transfer*, McGraw-Hill Book Company, New York, NY, 1972.
8. Walker, G., *Industrial Heat Exchangers A Basic Guide*, Hemisphere Publishing Corporation, New York, NY, 1982.
9. Kline, S.J., and McClintock, F.A., "Describing Uncertainties in Single-Sample Experiments", *Mechanical Engineering*, V.75, pp.3-8, January 1953.

INITIAL DISTRIBUTION LIST

		No. Copies
1.	Defense Technical Information Center Cameron Station Alexandria, Virginia 22304-6145	2
2.	Library, Code 0142 Naval Postgraduate School Monterey, California 93943-5002	2
3.	Chairman, Code 69He Mechanical Engineering Department Naval Postgraduate School Monterey, California 93943-5000	1
4.	Professor A. D. Kraus, Code 69Ks Department of Mechanical Engineering Naval Postgraduate School Monterey, California 93943-5000	2
5.	LTJG Ceyhun Cesur Dz. K. Komutanligi Okullar ve Kurslar Dairesi Bakanliklar, Ankara, Turkey	2
6.	Dz. K. Komutanligi Okullar ve Kurslar Dairesi Bakanliklar, Ankara, Turkey	5
7.	Deniz Harp Okulu Kutuphanesi Tuzla, Istanbul, Turkey	1
8.	Istanbul Teknik Universitesi Makine Fakultesi Kutuphanesi Istanbul, Turkey	1

126
17663/7
c

TITLE NUMBER: _____ CUSTOMER NUMBER: _____

LIBRARY: Dudley Knox Library, Naval Postgraduate School
Monterey, Ca 93943

ROSWELL BOOKBINDING

LIBRARY DIVISION

2614 NORTH 29th AVENUE
PHOENIX, ARIZONA 85009
PHONE (602) 272-9338

Binding in
Everything

☐

F B NP

CONTENTS

INDEX

Bind without Index

ISSUE CONTENTS

Discard

☐

Bind in Place

☐

Gather at Front

☐

IN OUT

Advertisements

Front Covers

Back Covers

1st only

Accents

Imprints

Special Instructions:

CEYHUN CESUR

C338415

Thesis C338415

Buck Color

Print Color

Trim Height

Ht Inches

Over Thick

For Title

Extra Lines

Extra Coll

Hand Sew

Slit

Rules

1st Slot No

Vol Slot No

Year Slot No

Call # Slot

Imp Slot No

Type Face

Price

Mending

Map Pockets

2 Vols in 1

598

Gold

ACTUAL TRIM

DATE

SPINE

JOB

BOARD DIM

LOT

CLOTH DIM

ROUTE

CLOTH BIN

SEQ NO

126
17668/7
C

220792

Thesis
C3384 C338415 Cesur
c.1 c.1

A correlation for the
heat transfer coefficient
in a rectangular passage
containing protuberance.

10 DEC 90

220792

Thesis
C338415 Cesur
c.1

A correlation for the
heat transfer coefficient
in a rectangular passage
containing protuberance.

thesC338415

A correlation for the heat transfer coef



3 2768 000 75630 8

DUDLEY KNOX LIBRARY